Study of the Couplings of QED and QCD from the Adler Function

Anthony Francis[a]**, Gregorio Herdoíza**[*b]**, Hanno Horch**[c]**, Benjamin Jäger**[d]**,
Harvey B. Meyer**[a,c]**, Hartmut Wittig**[a,c]

[a] *Helmholtz Institute Mainz,*
Johannes Gutenberg-Universität, 55099 Mainz, Germany

[b]*Instituto de Física Teórica UAM/CSIC and Departamento de Física Teórica,*
Universidad Autónoma de Madrid, Cantoblanco, E-28049 Madrid, Spain

[c] *PRISMA Cluster of Excellence, Institut für Kernphysik,*
Johannes Gutenberg-Universität, 55099 Mainz, Germany

[d] *Department of Physics, Swansea University, Swansea, United Kingdom*
E-mails: {francis,horch,meyerh,wittig}@kph.uni-mainz.de,
gregorio.herdoiza@uam.es, B.Jaeger@swansea.ac.uk

The contribution from hadronic vacuum polarisation effects is responsible for a large fraction of the theoretical uncertainty in the running of the QED coupling. The current level of uncertainty has become a limitation for electroweak precision tests. We use lattice QCD simulations with two flavours of O(a) improved Wilson fermions to determine the Adler function in a broad range of the momentum transfer Q^2. The running of the QED coupling, including valence contributions from u, d, s and c quarks, is compared to phenomenological results at intermediate Q^2 values. In the large Q^2 regime, the lattice determination of the Adler function is fitted to perturbation theory in order to examine the feasibility of a determination of the strong coupling constant.

---

[*]Speaker.

1. Introduction

The charge renormalisation in QED is due to the energy dependence induced by photon vacuum polarisation effects. The running of the QED coupling $\alpha(Q^2)$ can be written as follows,

$$\alpha(Q^2) = \frac{\alpha}{1 - \Delta\alpha_{\text{QED}}(Q^2)},$$ (1.1)

where α is the fine structure constant providing the classical charge normalisation at vanishing photon virtuality, $Q^2 = 0$. $\Delta\alpha_{\text{QED}}(Q^2)$ is related to the subtracted vacuum polarisation function (VPF). The relative size of the contributions to $\Delta\alpha_{\text{QED}}(Q^2)$ from loops of quarks and leptons is comparable. Recent determinations of $\alpha(Q^2)$ at $Q^2 = 0$ [1] and at the Z-boson mass [2] read,

$$\alpha = 1/137.035999074(44) \quad [0.3\,\text{ppb}],$$ (1.2)

$$\alpha(M_Z^2) = 1/128.952(14) \quad [10^{-4}],$$ (1.3)

where the values in brackets denote the relative error. While the central values shift by merely $\sim 6\%$, the errors instead deteriorate by five orders of magnitude when running up to the Z-pole. Hadronic effects are responsible for a large fraction of this loss of precision. A phenomenological approach [2–4] using dispersive methods together with experimental measurements of the cross-section, $\sigma(e^+e^- \to \text{hadrons})$, is at present used to measure the hadronic contribution to the running of the QED coupling, $\Delta\alpha_{\text{QED}}^{\text{had}}$. Lattice QCD provides an alternative method to determine this observable.

Contrary to the case of the lowest-order hadronic contribution to the anomalous magnetic moment of the muon, a_μ^{HLO}, which is dominated by the low-Q^2 regime, $\Delta\alpha_{\text{QED}}^{\text{had}}$ receives sizeable contributions from all energy regions. In order to run $\Delta\alpha_{\text{QED}}^{\text{had}}$ to the Z-boson mass, a matching to perturbative QCD (pQCD) is often done at $Q_{\text{match}}^2 \approx 6\,\text{GeV}^2$. At this energy scale, the dispersive approach tends to be poorly constrained by cross-section measurements in the region of s between 1 to $4\,\text{GeV}^2$ [5]. An interesting question is therefore to study whether there is a Q^2-interval where current lattice QCD calculations could reach a comparable accuracy than the dispersive approach. This would provide a valuable test in a context where the present error on $\Delta\alpha_{\text{QED}}$ has become a limitation for electroweak precision tests.

2. Lattice QCD Study of the Running of the QED Coupling

The hadronic vacuum polarisation tensor, depending on Euclidean momentum Q is given by,

$$\Pi_{\mu\nu}(\hat{Q}) = \int d^4x\, e^{iQx} \langle J_\mu(x) J_\nu(0) \rangle,$$ (2.1)

where, in practice, the lattice momentum $\hat{Q}_\mu = 2/a \sin(aQ_\mu/2)$ is used. The vector current reads,

$$J_\mu(x) = \sum_{f=u,d,s,c,\ldots} Q_f \overline{\psi}_f(x) \gamma_\mu \psi_f(x),$$ (2.2)

where Q_f is the electric charge of the quark flavour f. The VPF $\Pi(\hat{Q}^2)$ is extracted from,

$$\Pi_{\mu\nu}(\hat{Q}) = (\hat{Q}_\mu \hat{Q}_\nu - \delta_{\mu\nu} \hat{Q}^2) \Pi(\hat{Q}^2).$$ (2.3)

Ens.	a [fm]	V/a^4	M_{PS}	$M_{\mathrm{PS}}L$	N_{meas}
A3	0.079	64×32^3	473	6.0	1004
A4		64×32^3	363	4.7	1600
A5		64×32^3	312	4.0	1004
B6		96×48^3	267	5.1	1224
E5	0.063	64×32^3	456	4.7	4000
F6		96×48^3	325	5.0	1200
F7		96×48^3	277	4.2	1000
G8		128×64^3	193	4.0	820
N5	0.050	96×48^3	430	5.2	1392
N6		96×48^3	340	4.1	2236
O7		128×64^3	261	4.4	552

Table 1: Ensembles of O(a) improved Wilson fermions used in this work. Approximate values of the lattice spacing a and of the pion mass M_{PS} (in MeV) as well as information about the lattice volume and the number of measurements N_{meas} are provided.
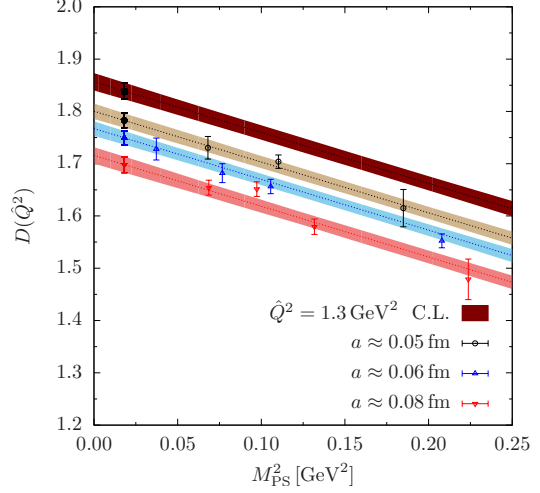

Figure 1: Pion mass dependence of the Adler function at fixed $\hat{Q}^2 = 1.3\,\mathrm{GeV}^2$. The upper band, denoted by 'C.L.', is the continuum limit estimate. The leftmost (filled) symbols indicate the extrapolated values at the physical pion mass.

The subtracted VPF, $\widehat{\Pi}(\hat{Q}^2) = \Pi(\hat{Q}^2) - \Pi(0)$, is directly related to the hadronic contribution to the running of the electromagnetic coupling, $\Delta\alpha_{\mathrm{QED}}^{\mathrm{had}}(\hat{Q}^2) = 4\pi\alpha\,\widehat{\Pi}(\hat{Q}^2)$. A related physical quantity that also allows to determine $\Delta\alpha_{\mathrm{QED}}^{\mathrm{had}}$ is the Adler function, defined in the following way,

$$D(\hat{Q}^2) \;=\; 12\pi^2\,\hat{Q}^2\,\frac{d\,\Pi(\hat{Q}^2)}{d\hat{Q}^2} \;=\; \frac{3\pi}{\alpha}\,\hat{Q}^2\,\frac{d}{d\hat{Q}^2}\Delta\alpha_{\mathrm{QED}}^{\mathrm{had}}(\hat{Q}^2). \tag{2.4}$$

The Adler function has a smooth dependence on $\hat{Q}^2$ due to the absence of resonance effects in the space-like domain. It is therefore a useful quantity to examine the $\hat{Q}^2$-regime where pQCD applies.

The calculation of $D(\hat{Q}^2)$ is based on a set of CLS lattice ensembles (c.f. table 1) with two flavours of O(a) improved Wilson fermions at three values of the lattice spacing and pseudoscalar meson masses down to 190 MeV satisfying the condition, $M_{\mathrm{PS}}L \geq 4$. The use of partially twisted boundary conditions [6] increases the density of $\hat{Q}^2$ values and allows to construct the Adler function from the numerical derivative of the VPF. We refer to refs. [7 – 9] for more details about our procedure to determine $D(\hat{Q}^2)$. The lattice data for $D(\hat{Q}^2)$ is parametrised by a fit ansatz that describes simultaneously the $\hat{Q}^2$ dependence through Padé approximants and the continuum and chiral extrapolations [8]. Once the parameters of these Padé approximants are known, it is possible to derive analytically the subtracted VPF, $\widehat{\Pi}(\hat{Q}^2)$. With respect to an approach where $\Pi(\hat{Q}^2)$ is directly used to determine $\Delta\alpha_{\mathrm{QED}}^{\mathrm{had}}$, a benefit of the Adler function in a global analysis of the lattice ensembles is that it requires significantly fewer fit parameters. Indeed, for each lattice ensemble, $\Pi(0)$ cancels in $D(\hat{Q}^2)$.

An illustration of the pion mass dependence of the (u,d) contribution to the Adler function – at fixed $\hat{Q}^2$ – is shown in Fig. 1. The coloured bands show the result of the global fit of the ensembles in table 1. In the momentum region, $\hat{Q}^2 \geq 1\,\mathrm{GeV}^2$, that is most useful for the determination of $\Delta\alpha_{\mathrm{QED}}^{\mathrm{had}}(\hat{Q}^2)$, we observe that the lattice data can be well described by a linear dependence on M_{PS}^2.
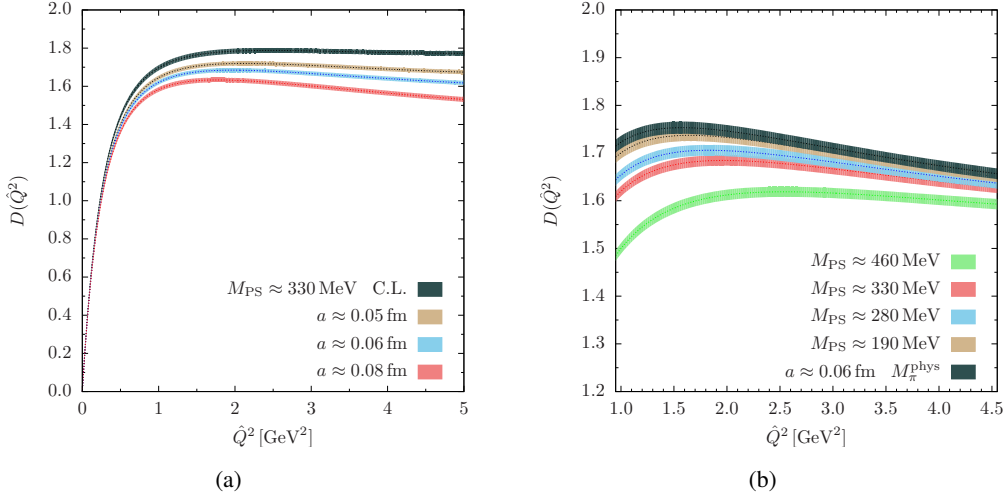
Figure 2: Dependence on the momentum $\hat{Q}^2$ of the (u,d) contribution to the Adler function. (a) The coloured bands indicate the lattice spacing dependence of $D(\hat{Q}^2)$ at a fixed pion mass, $M_{\rm PS} \approx 330\,{\rm MeV}$. The dark upper band, labelled 'C.L', is the continuum limit estimate. Cutoff effects are observed to grow for increasing values of $\hat{Q}^2$. (b) The effect of reducing the pion mass from $460\,{\rm MeV}$ down to $190\,{\rm MeV}$ is illustrated by the coloured bands. The dark upper band is the result of the extrapolation to the physical point. Light-quark mass effects are suppressed when increasing $\hat{Q}^2$.

We have repeated the analysis by excluding pion masses above $400\,{\rm MeV}$ to examine systematic effects in the chiral extrapolation. The $\hat{Q}^2$ behaviour of the (u,d) contribution to the Adler function is shown in Fig. 2. The size of lattice artefacts and of light quark mass effects – as a function of $\hat{Q}^2$ – can be inspected from the left and the right panels of Fig. 2, respectively.

Similar analyses were performed for the contributions to the Adler function from partially quenched strange s_Q and charm c_Q quarks. The results from the various flavour contributions to $D(\hat{Q}^2)$ in the continuum limit and at the physical point are presented in Fig. 3(a). The Adler function shows a substantial dependence on $\hat{Q}^2$ at the characteristic energy scale of QCD. For increasing values of $\hat{Q}^2$, we observe a clear separation among the various flavour contributions and the approach towards the pQCD behaviour.

Preliminary results for the running of the QED coupling are shown in Fig. 3(b). When increasing the flavour content up to the inclusion of (u,d), s_Q and c_Q contributions, the lattice result approaches the five-flavour result from a phenomenological analysis based on the dispersive approach. The bands in Fig. 3(b) refer to lattice results in the continuum and at the physical point with uncertainties that are purely statistical. While a detailed comparison of lattice and phenomenological results – together with a complete account of systematic effects – is in progress, it is already interesting to note that the statistical errors from the lattice are comparable to those of the dispersive approach for $Q^2 \gtrsim 1\,{\rm GeV}^2$. This is contrast with the behaviour in the low-Q^2 region – which is most relevant for $a_\mu^{\rm HLO}$ – where the lattice data is affected by larger fluctuations. We note that differences and ratios of $\Delta\alpha_{\rm QED}^{\rm had}$ between two different scales can be built to further reduce the overall uncertainties. There are, therefore, good prospects for an accurate determination of $\Delta\alpha_{\rm QED}^{\rm had}$ from lattice QCD.
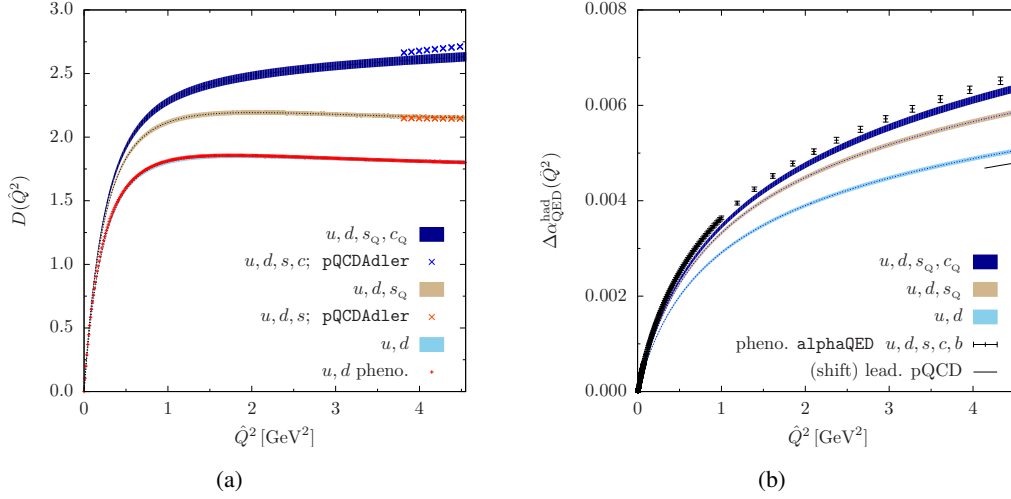
(a)   (b)

Figure 3: (a) Contributions from (u,d) and from partially quenched strange s_Q and charm c_Q quark flavours to $D(\hat{Q}^2)$ after having performed the continuum and chiral extrapolations. The (u,d) contribution is consistent with the phenomenological model of ref. [10] denoted by the red '+' symbols. For the cases where s_Q and c_Q are included, perturbative QCD (pQCD) results from the `pQCDAdler` package [11] are also shown. (b) Hadronic contribution to the running of the QED coupling for (u,d), s_Q and c_Q quark flavours. The five-flavour result from the dispersion relation approach – implemented in the package `alphaQED` [3, 11] – is shown by the black data points. The leading-order pQCD result for the (u,d) case is shown by a small continuous black line that was shifted vertically to improve the visibility. The lattice error bands denote the size of statistical uncertainties only.

3. Matching of the Adler Function to pQCD

The Adler function is a useful quantity to monitor the regime of momenta where pQCD is applicable. Non-perturbative effects can be incorporated in the pQCD expansion through an operator product expansion (OPE) where the operator matrix elements capture the long-range strong interaction effects while the perturbative Wilson coefficients encode the short distance physics. The matching of a lattice determination of $D(\hat{Q}^2)$ to its OPE counterpart has to be performed at large enough $\hat{Q}^2$ values to guarantee the convergence of the pQCD expansion. However, lattice artefacts increase with $\hat{Q}^2$ and should therefore fulfil the condition, $(a\hat{Q})^2 \ll 1$, to be kept under control. A first account of our investigations about the possibility to determine Λ_{QCD} from a matching to pQCD of the VPF evaluated on the lattice was reported in [12].

Non-singlet contributions to $D(Q^2)$ are considered both on the lattice and the pQCD sides. The OPE of the Adler function reads,

$$D_{\mathrm{OPE}}(Q^2, \alpha_s, m_{\mathrm{f}}) = D_0(\alpha_s, Q^2, \mu^2) + D_2^m(\alpha_s, Q^2, \mu^2) \frac{\left(\overline{m}_{\mathrm{f}}[Q^2]\right)^2}{Q^2} + D_4^{\mathrm{F}}(\alpha_s, Q^2, \mu^2) \frac{\overline{m}_{\mathrm{f}} \langle \bar{\psi}_{\mathrm{f}} \psi_{\mathrm{f}} \rangle}{Q^4}$$

$$+ D_4^{\mathrm{G}}(\alpha_s, Q^2, \mu^2) \frac{\langle O_{\mathrm{OPE}}^{(4)} \rangle}{Q^4} + \mathcal{O}\left(\frac{1}{Q^6}\right), \tag{3.1}$$

where the flavour content, $\mathrm{f} = (u,d)$, is considered. The Wilson coefficients D_0, D_2^m, D_4^{F} and D_4^{G} in eq. (3.1) are computed in pQCD and, depending on the case, are known from 1- to 4-loop order in
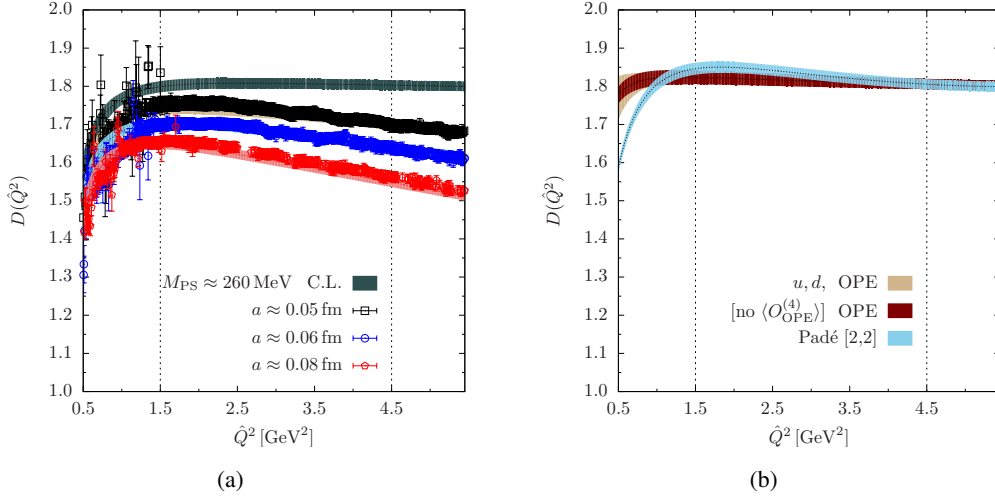
5

Figure 4: Dependence on the momentum $\hat{Q}^2$ of the (u,d) contribution to the Adler function. (a) The lattice data from ensembles at three different values of the lattice spacing and $M_{PS} \approx 260\,\text{MeV}$ are fitted to an OPE expression in eq. (3.1) supplemented with terms parametrising lattice artefacts. The dark upper band, labelled 'C.L', is the continuum limit estimate. (b) Comparison of the use of OPE and Padé ansätze in the determination of the Adler function after having performed the continuum and chiral extrapolations. Signs of compatibility are observed only at sufficiently large $\hat{Q}^2$ values, where the perturbative series is better behaved. The effect of removing from the OPE the contribution for the dimension-four condensate is also shown. In both panels, the $\hat{Q}^2$-interval considered in the OPE fit is denoted by the vertical dashed lines and the bands denote statistical errors only.

the α_s expansion [13 – 15]. Non-perturbative effects are encoded through the condensates $\langle \overline{\psi}_f \psi_f \rangle$ and $\langle O_{OPE}^{(4)} \rangle$. The pQCD expressions are defined in the $\overline{\text{MS}}$ scheme. The connection of the coupling α_s to the scale $\Lambda_{\overline{MS}}^{(N_f=2)}$ is given by the 4-loop β-function [16]. The renormalised quark mass $\overline{m}_f(\mu^2)$ is given at the renormalisation scale μ [17, 18]. Since the Adler function is a physical quantity, any residual scheme and scale dependence should vanish as higher order terms are included.

The measurements of $D(\hat{Q}^2)$ from the complete set of ensembles in table 1 are matched to the OPE expression in eq. (3.1) where $\alpha_s(\mu = 2\,\text{GeV})$ and $\langle O_{OPE}^{(4)} \rangle$ are left as fit parameters. The fit ansatz is augmented by two terms parametrising $\hat{Q}^2$-dependent and -independent discretisation effects, respectively. For the RGI product, $\overline{m}_f \langle \overline{\psi}_f \psi_f \rangle$, we use as input the value of the chiral condensate, $\langle \overline{\psi}_u \psi_u \rangle = -(0.269(8)\,\text{GeV}^3)$ [19].

Fig. 4(a) shows an example of an OPE fit from $1.5 - 4.5\,\text{GeV}^2$ that confirms that a proper control of lattice artefacts is essential for the matching to pQCD. The continuum estimate of $D(\hat{Q}^2)$ based on Padé approximants (c.f. sect. 2) can be compared to the results of the OPE fit. This is illustrated in Fig. 4(b), where the effect of removing the $\langle O_{OPE}^{(4)} \rangle$ term in eq. (3.1) is also shown. In the $\hat{Q}^2$-interval, $1.5 - 4.5\,\text{GeV}^2$, where the OPE fit is performed, deviations at the two-sigma level can be observed – based on statistical errors only. The expected breakdown of the perturbative expansion is manifest for lower $\hat{Q}^2$ values. Barring yet uncontrolled systematic effects, Fig. 4(b) suggests that momenta, $Q^2 \gtrsim 4\,\text{GeV}^2$, might be needed to observe reliable signs of convergence of the pQCD expansion of the Adler function.

Conclusions

The electromagnetic coupling is an input parameter in a number of precision studies of the Standard Model. An accurate determination of its running is essential to constrain many of these processes. Our studies provide evidences for the potential advantage of a lattice calculation of the Adler function $D(Q^2)$ to achieve a rather precise determination $\Delta\alpha_{\mathrm{QED}}^{\mathrm{had}}(Q^2)$. Furthermore, a comparison of $D(Q^2)$ to an approximation based on the OPE suggests that momenta, $Q^2 \gtrsim 4\,\mathrm{GeV}^2$, are needed to observe reliable signs of convergence of the perturbative expansion. Ongoing studies will provide a more complete account of the systematic effects present in these determinations.

References

[1]　K. A. Olive *et al.* [PDG Collaboration], Chin. Phys. C **38** (2014) 090001.

[2]　M. Davier *et al.*, Eur. Phys. J. C **71** (2011) 1515 [Erratum-ibid. C **72** (2012) 1874].

[3]　F. Jegerlehner, Nuovo Cim. C **034S1** (2011) 31 [arXiv:1107.4683].

[4]　K. Hagiwara *et al.*, J. Phys. G **38** (2011) 085003 [arXiv:1105.3149].

[5]　F. Jegerlehner, Nucl. Phys. Proc. Suppl. **181-182** (2008) 135 [arXiv:0807.4206].

[6]　M. Della Morte, B. Jäger, A. Jüttner and H. Wittig, JHEP **1203** (2012) 055 [arXiv:1112.2894].

[7]　H. Horch *et al.*, PoS LATTICE **2013** (2013) 304 [arXiv:1311.6975].

[8]　M. Della Morte *et al.*, PoS LATTICE **2014** (2014) 162 [arXiv:1411.1206].

[9]　A. Francis *et al.*, [arXiv:1411.3031].

[10]　D. Bernecker and H. B. Meyer, Eur. Phys. J. A **47** (2011) 148 [arXiv:1107.4388].

[11]　http://www-com.physik.hu-berlin.de/∼fjeger/software.html

[12]　G. Herdoíza, H. Horch, B. Jäger and H. Wittig, PoS LATTICE **2013** (2014) 444.

[13]　K. G. Chetyrkin, J. H. Kühn and M. Steinhauser, Nucl. Phys. B **482** (1996) 213 [hep-ph/9606230].

[14]　P. A. Baikov, K. G. Chetyrkin, J. H. Kühn and J. Rittinger, JHEP **1207** (2012) 017 [arXiv:1206.1284].

[15]　K. G. Chetyrkin, V. P. Spiridonov and S. G. Gorishnii, Phys. Lett. B **160** (1985) 149.

[16]　T. van Ritbergen *et al.*, Phys. Lett. B **400** (1997) 379 [hep-ph/9701390].

[17]　P. Fritzsch *et al.* [ALPHA Collaboration], Nucl. Phys. B **865** (2012) 397 [arXiv:1205.5380].

[18]　K. G. Chetyrkin and A. Retey, Nucl. Phys. B **583** (2000) 3 [hep-ph/9910332].

[19]　S. Aoki *et al.* [FLAG Working Group], Eur. Phys. J. C **74** (2014) 9, 2890 [arXiv:1310.8555].